Supporting Information for "Aquatic exposures and downstream mass loading of per- and poly-fluoroalkyl substances (PFAS), including trifluoroacetic acid (TFA), caused by groundwater contaminant plumes of historic landfills"

by J.W. Roy[1]*, V.R. Propp[2], T. Hua[2], S.J. Brown[1], C. Brinovcar[1], J.E. Smith[2], A.O. De Silva[1]

Appendix A: Images of Study Site

Appendix B: Monitoring Locations at the Study Sites

Appendix C: Additional Method Details

Appendix D – Additional Site Characterization

Appendix E - Additional Non-landfill Observations

Appendix A: Images of Study Site

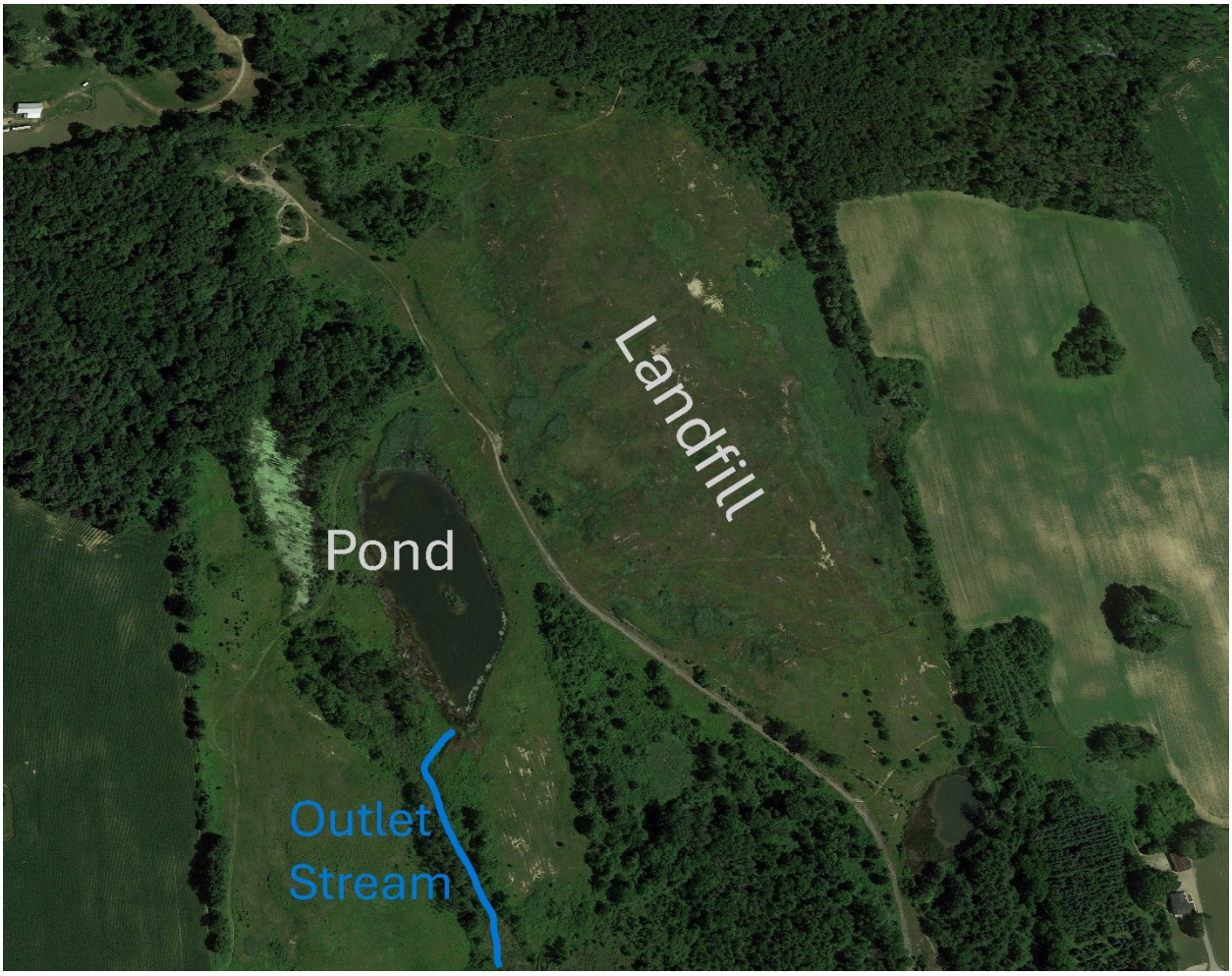

Figure S1. Satellite photo of the HB site, showing the single large landfill and the receiving pond to the west.

Figure S2. Satellite photo of the DC site with its three landfills (A, B, C) situated along Dyment's Creek (flowing west; right).

Figure S3. Picture of upstream discharge gauging location (DC-U) for DC site during winter. Note the snow piles on shores due to the plowing of snow from an uphill parking lot towards the right of the image (not shown).

Figure S4. Picture of downstream discharge gauging location (DC_D) for DC site during summer. Note upstream road culvert and debris throughout stream.

(A)

Figure S5. DC Site: Stretch B during (A) summer base flow and (B) a high flow precipitation event on October 16th, 2019.

(A)

Figure S6. DC Site: Stretch C during (A) summer base flow and (B) a high flow precipitation event on October 16th, 2019.

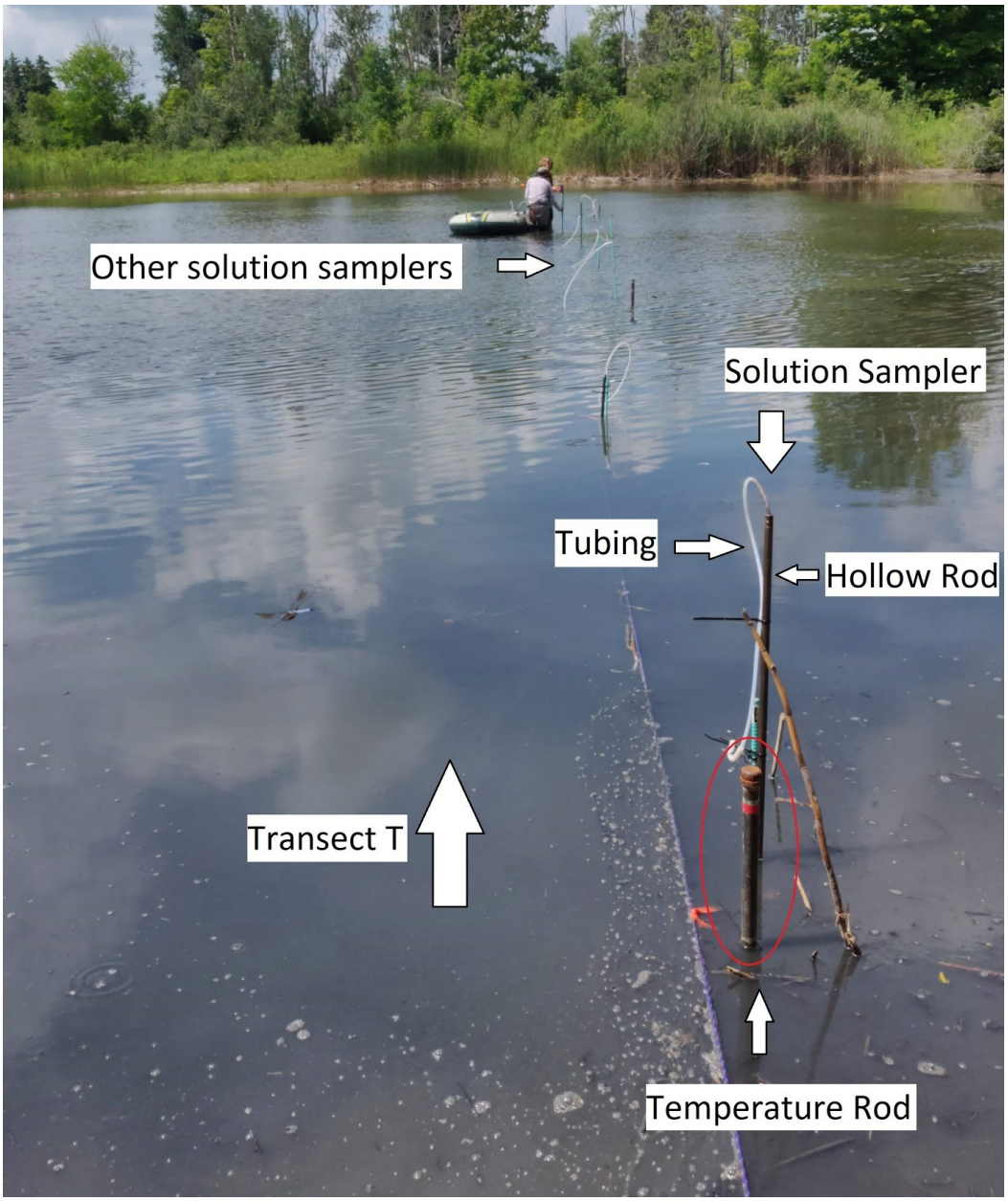

Figure S7. Photo of Transect E-W at the HB Site and some of its semi-permanent solution samplers. Solution sampler's metal hollow rod is sticking out of the pond surface, along with tubing that attaches to a peristaltic pump.

Appendix B: Monitoring Locations at the Study Sites

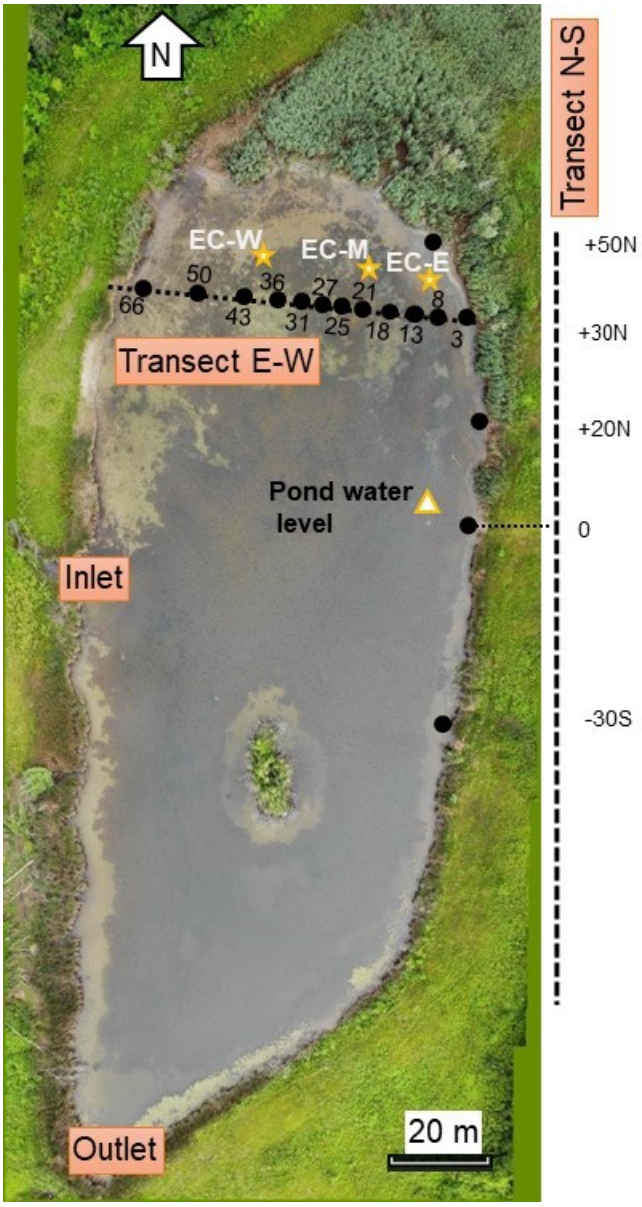

Figure S8. Birds-eye view of the HB Site's pond, indicating the two sampling transects with shallow groundwater sampling locations (black circles) and the three locations of the epibenthic continuous EC and temperature monitoring at 1 cm above the pond sediment (stars). The site landfill is to the east.

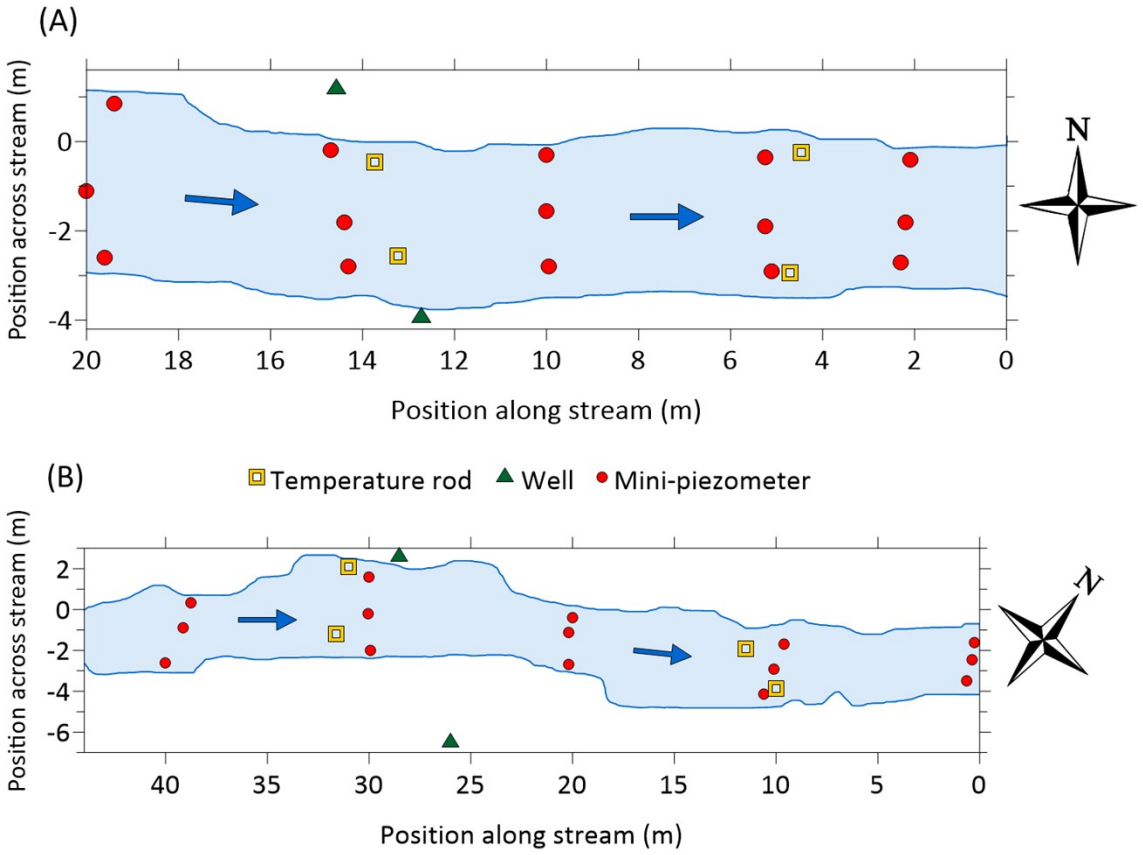

Figure S9: General layout of the instrumentation beside and within the stream (blue, arrows indicate flow direction) at the DC Site's Stretch B (A) and Stretch C (B). Shallow groundwater sampling was performed from the mini-piezometers (with PFAS samples only from the south bank in (A) and north bank in (B)).

Appendix C: Additional Method Details

Table S1. List of compounds analyzed for each sampling suite.

Artificial Sweeteners	Acesulfame, Saccharin, Cyclamate, Sucralose, Perchlorate, Glyphosate, 2,4-D, Fosamine, MCPA, Picloram, Sulfamic Acid
Anions	Fluoride, Chloride, Nitrite, Bromide, Sulfate, Nitrate
Cations	Calcium, Magnesium, Potassium, Silica, Sodium
Dissolved Metals	Antimony, Arsenic, Barium, Beryllium, Bismuth, Boron, Cadmium, Cerium, Cesium, Chromium, Cobalt, Copper, Gallium, Iron, Lanthanum, Lead, Lithium, Manganese, Molybdenum, Nickel, Niobium, Platinum, Rubidium, Selenium, Silver, Strontium, Thallium, Tin, Titanium, Tungsten, Uranium, Vanadium, Yttrium, Zinc
Volatile Organic Compounds	Chloromethane, vinyl chloride, bromomethane, chloroethane, diethylether, carbon disulfide, CFC-113, iodomethane, allyl chloride, methylene chloride, *trans*-1,2-dichloroethene, acetonitrile, chloropropene, 1,1-dichloroethane, acrylonitrile, *cis*-1,2-dichloroethene, dichloropropane, chloroform, carbon tetrachloride, 1,1,1-trichloroethane, tetrahydrofuran, 1,1-dichloropropene, benzene, methylacrylonitrile, 1,2-dichloroethane, trichloroethene, dibromomethane, 1,2-dichlropropane, bromodichloromethane, methyl methacrylate, cis-1,3 dichloropropene, toluene, nitropropane, tetrachloroethene, trans-1,3-dichloropropene, 1,1,2--trichloroethane, ethyl methacrylate, dibromochloromethane, 1,3-dichloropropane, 1,2-dibromomethane, chlorobenzene, ethyl benzene, 1,1,1,2-tetrachloroethane, m+p-xylene, o-xylene, styrene, bromoform, isopropyl benzene, bromobenzene, n-propylbenzene, 1,1,2,2-tetrachloroethane, 2-chlorotoluene, 1,3,5-trimethylbenzene, 1,2,3-trichloropropane, trans-1,4-dichloro-2-butene, 4-chlorotoluene, tert-butylbenzene, pentachloroethane, 1,2,4-trimethylbenzene, sec-butylbenzene, p-cymene, 1,3-dichlorobenzene, 1,4-dichlorobenzene, n-butylbenzene, 1,2-dichlorobenzene, 1,2-dibromo-3-chloropropane, nitrobenzene, hexachlorobutadiene, 1,2,4-trichlorobenzene, naphthalene, 1,2,3-trichlorobenzene
Per and polyfluoroalkyl substances (PFAS)	see Table 1

Table S2. Details on sample containers, preservation, and storage. (PE – polyethylene)

Analysis	**Filtered? (0.45-µm)**	**Preservation**	**Bottle Type and Volume**	**Storage**
SC/LC PFAS suite	N	None	PE 500mL- methanol rinsed	Fridge 4°C
Artificial sweeteners / USC-PFAS	Y		PE 20mL	Freezer
Ammonium-N	Y	10% HCl until pH 5-6	PE 20mL	Freezer
Metals / major cations	Y	70% HNO_3 until pH<2	PE 30mL or 120mL	Fridge 4°C
VOCs	N	$NaHSO_4$ crystals, no head space	Glass 40mL	Fridge 4°C
Anions	Y		PE 20mL	Fridge 4°C
SRP	Y		Glass 40mL	Fridge 4°C
Alkalinity	N		PE 120mL	Fridge 4°C

C1. Method for Ultra Short Chain (USC) PFAS by IC/MS/MS

High purity chemicals were used to prepare standards. Trifluoroactetic acid (TFA) was purchased from Sigma-Aldrich Canada Ltd. (Oakville, ON, Canada). The 2,2,3,3,3 pentafluoropropanoic acid (PFPrA), trifluoromethane sulfonic acid (TFMS), sodium salt of perfluoropropane sulfonic (PFPrS) were purchased from Toronto Research Chemicals (Toronto, ON, Canada). Perfluorobutanoic acid (PFBA) was purchased from Wellington Laboratories (Guelph, ON, Canada). Isotopically labelled internal standards for TFA-$^{13}C_2$, PFPrA-^{13}C and acesulfame-d4 potassium were from Toronto Research Chemicals (Toronto, ON, Canada), PFBA-^{13}C3 was from Wellington Laboratories, and saccharin-^{13}C6 and perchlorate-^{18}O4 were from Cambridge Isotopes (Andover, MI, USA). Isotopically labelled PFPrS and TFMS were not available. Optima LC/MS grade methanol was obtained from Fisher Scientific (Suwanee, GA, USA). All water used was reverse osmosis water treated with a Milli-Q (MQ) Gradient system to produce <18.2 µS water. Standards were made by dissolving the high purity chemicals in MQ treated water and diluting with MQ treated water to the appropriate concentration.

The instruments used to analyze USC PFAS were a Thermo Scientific 5000 ion chromatography (IC) system (Waltham, Massachusetts, USA) coupled to a QTRAP 5500 (AB Sciex, Concord, ON, CAN) triple-quadrupole mass-spectrometer. The Thermo Scientific 5000 IC system included the following components: AS-AP auto-sampler, ICS-5000 DP analytical flow pump, ICS 5000 eluent generator, conductivity detector in an ICS-5000 DC detector compartment, AERS 500 2mm suppressor, IONPAC® AS20 analytical column (2 x 250 mm) and an IONPAC® AG20 guard column (2 x 50 mm). An AXP isocratic pump delivered MQ water at 1.2 ml/min to the suppressor to ensure a background conductivity of < 1 µS. Background conductivity was typically less than 0.5 µS. A potassium hydroxide gradient eluent was run from 10 mM to 75 mM at a flow rate of 0.35 mL/min (10 mM for first 5 minutes, ramped to 50 mM over 1 min, held at 50 mM for 6 min, ramped to 75 mM over 1 min, held at 75 mM for 5 min, then brought back to 10 mM). The suppressor current was maintained at 66 mA. The IC system was run using Chromeleon 6.8. Retention times were as follows: TFA 6.8 min, PFPrA 7.3 min, PFBA 8.2 min, TFMS 10.3 min and PFPrS 12.4 min. The retention time for labeled isotopes matched the native retention times. Retention times for the internal standard surrogates (acesulfame d-4 and perchlorate $^{18}O4$) were 10.97 and 14.0, respectively.

A 1200 series Agilent (Santa Clara, CA, USA) isocratic pump was used to tee in 0.2 ml/min of methanol with the IC effluent at the mass spectrometer source. Total flow into the mass spectrometer was 0.55 mL/min. Injection volume was 100 µL. The QTRAP 5500 triple quadrupole mass spectrometer was operated in negative electrospray ionization (ESI) mode, using Analyst® version 1.6.3. The following conditions were found to provide the optimum signal for analyses: curtain gas 35 arbitrary units (a.u.), ionspray voltage -3000 V, source temperature 700°C, nebulizer gas 60 a.u., heater gas 60 a.u., and collision gas 12 a.u. Where available, two multiple reaction monitoring (MRM) transitions were monitored for each analyte and one for each isotope labeled internal standard (Table S3).

Table S3. Analyte retention time minutes (RT), Quantification (Quan) and Qualification (Qual) multiple reaction monitoring (MRM) transitions of parent (Q1) and product (Q3) ion with declustering potential (DP) and collision energy (CE) applied. Note that i.s. identifies the internal standards.

Analyte (RT)	**Q1**	**Q3**	**DP**	**CE**
TFA (6.8)				

Quan	112.8	68.9	-30	-17
i.s. TFA ^{13}C-2	115	70	-30	-17
PFPrA (7.3)				
Quan	162.9	119.2	-30	-15
Qual	162.9	69	-30	-47
i.s. PFPrA ^{13}C	164	119	-30	-15
PFBA (8.2)				
Quan	213	169	-25	-13
i.s. PFBA ^{13}C-3	216	172	-25	-13
TFMS (10.3)				
Quan	148.9	79.9	-80	-23
Qual	148.9	98.9	-80	-35
i.s. acesulfame d-4 (10.97)	166	86	-44	-22
PFPrS (12.4)				
Quan	248.9	79.9	-80	-50
Qual	248.9	99	-80	-35
i.s. ClO4 ^{18}O4 (14.0)	107	89	-115	-39

Detection Limits:

Eight consecutive injections of a standard solution that had a signal-to-noise ratio <25 were used to calculate the method detection limit (MDL) as follows: the MDL was estimated as the product of the standard deviation and the student t-value for n-1 degrees of freedom. The practical quantitation level (PQL) was calculated as 3 times the MDL. MDL could not be calculated for PFPrA due to background levels. See Table S4 for results.

Table S4. Method detection limit (MDL) and practical quantification limit (PQL) based on 8 consecutive injections of USC PFAS ng/L. **the PQL is less than the lowest standard in the curve so reporting PQL is equal to the lowest standard (2.5 ng/L).

Injection #	TFA (S/N 10) ng/L	PFBA (S/N 19) ng/L	TFMS** (S/N 23) ng/L	PFPrS **(S/N 7) ng/L
1	244.7	66.6	2.5	2.6
2	244.0	61.5	2.6	2.4
3	261.4	60.6	2.7	2.6
4	249.7	63.8	2.5	2.5
5	235.2	60.8	2.7	2.2
6	249.3	64.6	2.6	2.7
7	248.6	57.7	2.5	2.6
8	256.3	59.7	2.6	2.4
variance (S2)	62.5	8.3	0.004	0.029
std dev (S)	7.9	2.9	0.1	0.2
t	3.0	3.0	3.0	3.0
MDL (S*t), ng/L	23.7	8.6	0.2	0.5
PQL (3*MDL), ng/L	71.1	25.9	0.6	1.5
average	248.6	61.9	2.6	2.5
Relative standard deviation (% RSD)	3.2	4.7	2.5	6.8

Quantitation:

A standard curve was created with a minimum of 6 points (maximum of 8) covering the range from the minimum detection limit for each analyte up to 2000 ng/L. All standard curves included a concentration less than the PQL. Matrix effects and instrument variations were corrected by internal standard response. All standard curves were quadratic regressions weighted $1/x^2$ and the correlation coefficients (R^2) of the regression equations were all greater than 0.995. See Table S5. The area of the most sensitive MRM transition for each analyte was used for concentration calculations and the second transition was used to confirm compound identification. Samples with concentrations greater than the highest standard were diluted with Milli-Q water to be within the calibration curve range and were re-run.

Recovery:

Tests were conducted to determine the recovery of analytes under high ionic strength conditions that could potentially occur in some groundwater. An artificial groundwater (AGW) was made with equal amounts (100 mg/L each) of the anions chloride, carbonate and sulfate. Then 2000 ng/L of each USC PFAS analyte was added to the 100 mg/L AGW and % recovery calculated. Percent recoveries in AGW range from 102.5% to 111.4% with an average of 107.3%. See Table S5 for results.

Table S5. USC PFAS standard curve ranges, isotopically labelled internal standard used to account for instrument variation and matrix effects, coefficient of determination (r^2) and % recovery in AGW.

Analyte	Std range ng/L	internal standard	r^2	% Recovery
TFA	62.5 to 2000	TFA ^{13}C-2	0.99734	111.4
PFPrA	12.5 to 2000	PFPrA ^{13}C	0.99922	105.7
PFBA	12.5 to 2000	PFBA ^{13}C-3	0.99969	102.5
TFMS	2.5 to 2000	Ace d-4	0.99929	103.8
PFPrS	2.5 to 2000	ClO4 ^{18}O4	0.99908	113.1

QA/QC:

To achieve a positive identification, the retention time match of the native and labeled analyte had to be within 2% and, if available, the calculated concentration of the two MRM transitions had to be within

20% of each other for levels > PQL. After every 10 samples run, a duplicate and a check standard were analysed. Duplicates and check standards quantitative MRM were required to be within +/- 20% of the expected value for levels > PQL and within +/- 50% for levels >MDL and <PQL.

C2. Details on Analysis of Short chain and Long chain Per- and Polyfluoroalkyl Substances: We have previously reported our methods for PFAS extraction from aqueous matrices using weak-anion exchange (WAX) solid phase extraction (SPE) (MacInnis et al. 2019). Briefly, a 200 ml subsample of groundwater was brought up to room temperature, spiked with isotopically labeled standards (for extraction efficiency) and adjusted to pH 3 using acetic acid. The sample is loaded onto a 150 mg WAX SPE (Waters, Mississauga, ON) that was conditioned using 5 ml 0.1% ammonia in methanol, 5 ml methanol and 5 ml of SPE-polished HPLC-grade water. Once the sample has passed through the SPE, the cartridge is dried by centrifugation. A fractional elution is used to collect neutral PFAS using 6 ml methanol and anionic PFAS using 8 ml 0.1% ammonia in methanol. Both fractions are brought to dryness using a gentle stream of nitrogen and reconstituted in 0.5 ml 1:1 methanol/water with an additional spike of a separate cocktail of isotopically labeled standards to evaluate matrix effects. Extracts are transferred to 300-µl polypropylene vials for analysis by ultra high performance liquid chromatography tandem mass spectrometry (UHPLC-MS/MS, Waters Acquity UHPLC and Waters Acquity TQS MS/MS). Analytes are separated using an octadecylsilyl (C18) column with an upstream isolator column to separate any background PFAS signal. All mass spectrometry parameters including cone voltage and collision energies for precursor to product ion transitions were optimized using authentic standards and are available in previous publications (MacInnis et al. 2019). All analytes were quantified using a 16-level calibration curve ranging from 0.01 to 15 ng/ml, R^2>0.99. Quantitation was based on relative response to the corresponding isotopically labeled standard to correct for recovery and matrix effects. For extracts yielding concentrations outside of the calibration curve, dilution was performed for reanalysis.

QA/QC parameters included method blanks, sample spike and recovery, comparison of field and travel blanks. Method detection limits were based on the average + 3 standard deviation concentration of the blanks. For analytes not detected in the method blank, the MDL is based on a standard injection yielding a signal-to-noise ratio of 3. Extraction efficiency was based on the analyte peak area in the extract of a spiked sample compared to a sample extract that was spiked post-extraction. Extraction efficiencies for all PFCAs with 4 to 11 carbons corresponded to 102 ± 3%. For PFCA with 12 or more carbon atoms, extraction efficiencies were 70 ± 4%. For all PFSA, extraction efficiencies were 107± 8%. Method detection

limits were based on instrument detection limits (concentrations yielding a signal to noise ratio of 3) multiplied by the concentration factor.

C3. Further Details on Analysis of Artificial Sweeteners:

The artificial sweeteners suite was determined by Ion Chromatography coupled to a tandem mass spectrometer as for the USC-PFAS analysis. Two MRM transitions were monitored and quantification was performed using deuterated compounds to correct for matrix effects and instrument fluctuations. Positive identification required the retention time match of the native and labeled analyte to be < 2% and the calculated concentration of the two MRM transitions to be < 20% of each other for values > PQL. Duplicate and a check standard were run after every 10 samples, with quantitative MRM required to be within +/- 20% of the expected value for levels > PQL and within +/- 50% for levels >mdl (minimum detection limit) and <PQL. Accuracy and precision were assessed by injecting the third lowest standard 7 times over a 96-hour period of a sample run. The average % recovery and % standard deviation were required to be 100 +/- 20 % and <10%, respectively. For each analyte, a standard curve was created with a minimum of 5 points over a range of approximately 3 orders of magnitude. Complete instrument details can be found in Van Stempvoort et al. (2020) with MRM details and compound specific parameters for saccharin reported in Van Stempvoort et al. (2019). MDL and PQL for saccharin were 2 and 6 ng/L, respectively.

C4. Methods for Additional Chemical Analyses:

Soluble reactive phosphorus (SRP) was measured with a Thermo Scientific Evolution 160 spectrophotometer using a mixed reagent of ammonium molybdenate and antimony potassium tartate (absorbance measured at 885nm). A set of 71 VOCs, largely chlorinated solvents and petroleum compounds, were analyzed with a Teledyne Tekmar Aquatek 70 autosampler, a Teledyne Tekmar 3100 sample concentrator purge and trap, an Agilent G1530A gas chromatograph, and a HP/Agilent 5973 mass selective detector. Trace metals and cations were analyzed using Inductively Coupled Plasma-Sector Field Mass Spectrometry (ICP-MS, NLET method #2003) at the National Laboratory for Environmental Testing. Alkalinity was analyzed using HACH digital titration method 8203 with 1.6 N H_2SO_4.

Appendix D: Additional Site Data

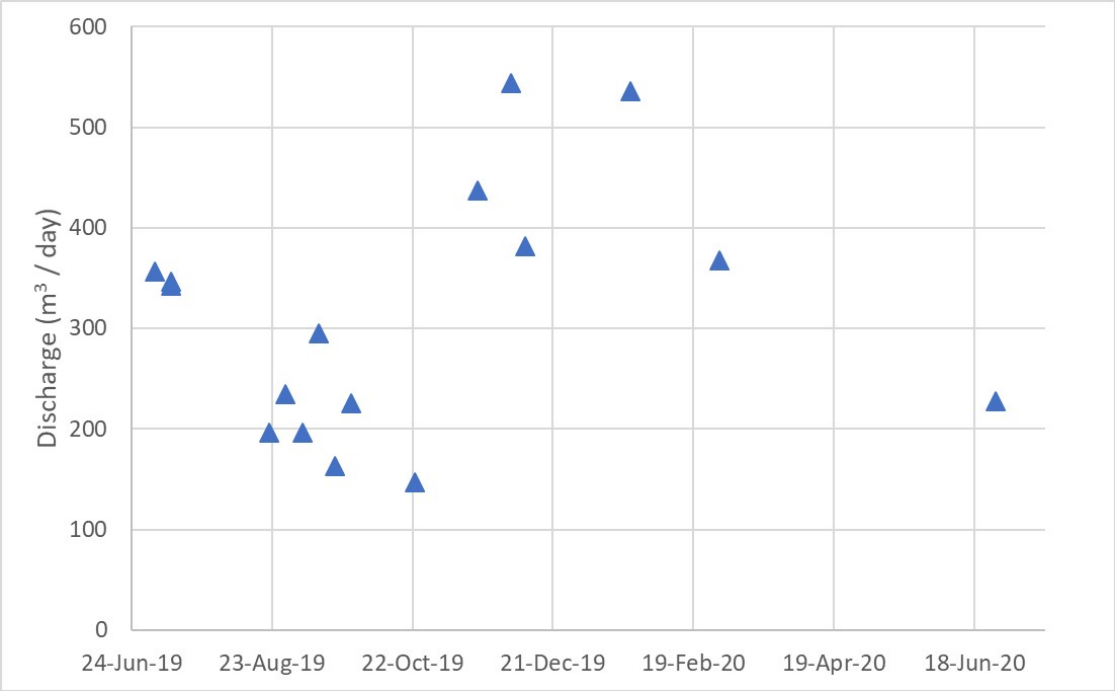

Figure S10. Pond outlet stream discharge measurements made at the culvert, noting that the percent error in the discharge measurements could range to 15-20%.

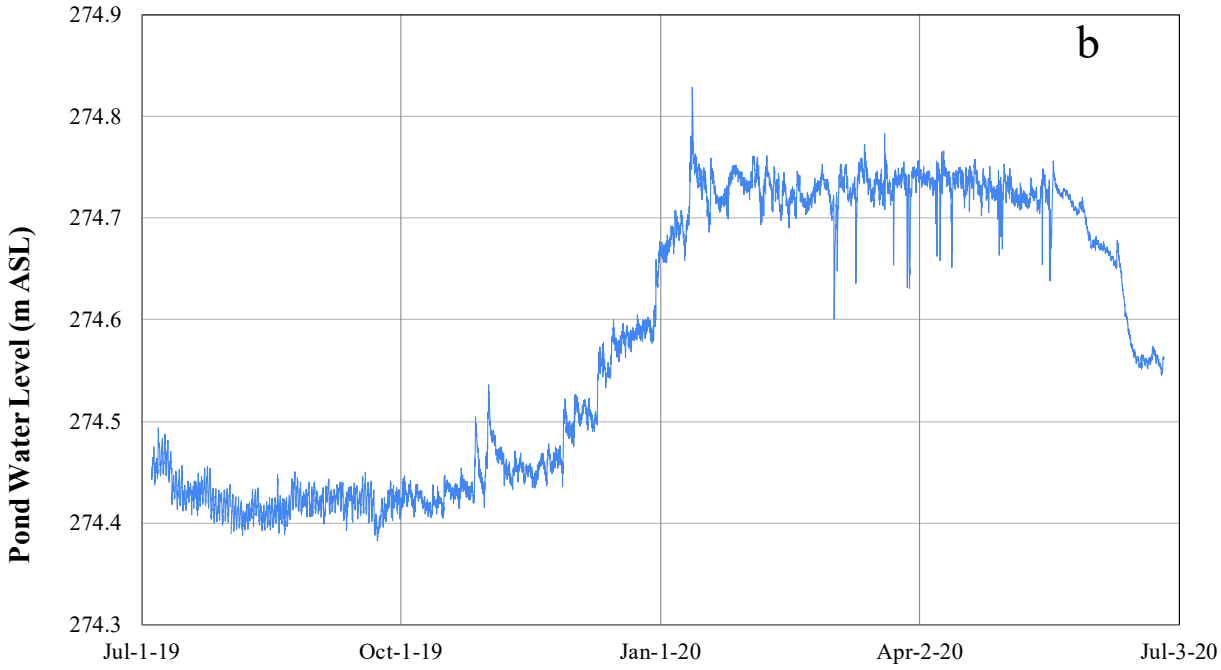

Figure S11. HB site pond water level. Sharp dips in water level data in March and April 2020 are due to problems with barometric pressure compensation resulting from snow covering the air holes of the sensor housing.

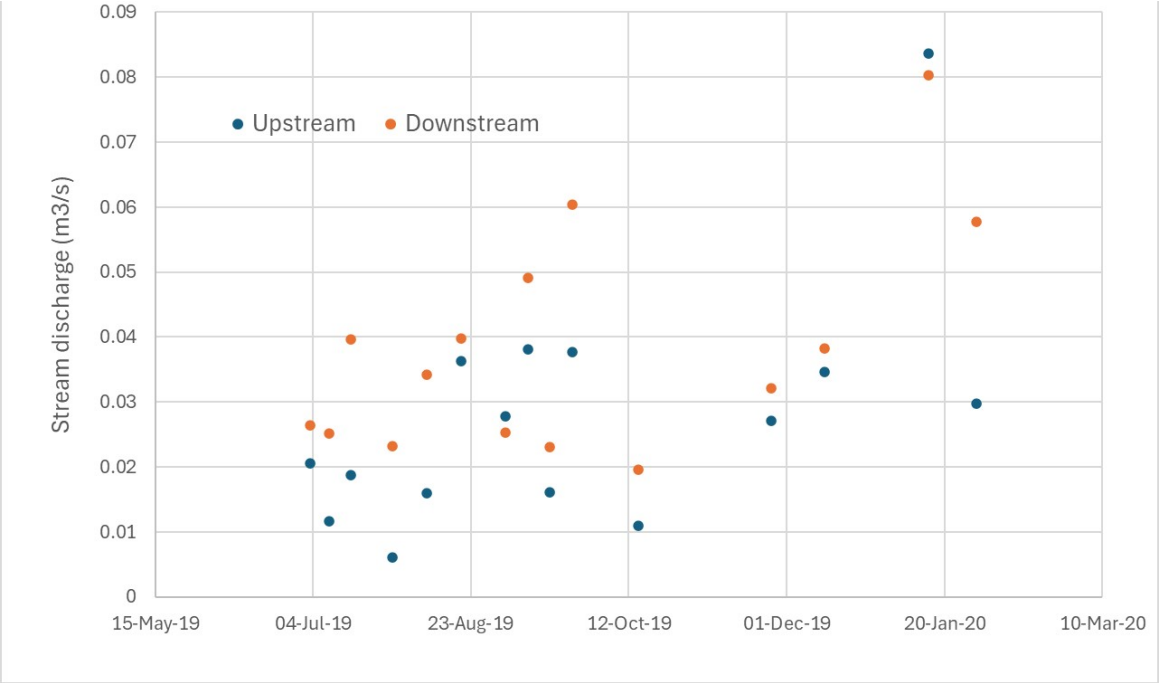

Figure S12. Stream discharge at the DC site at the upstream (DC-U) and downstream (DC-D) locations (Fig. 1) over the study period. Higher values downstream indicate inputs from groundwater discharge.

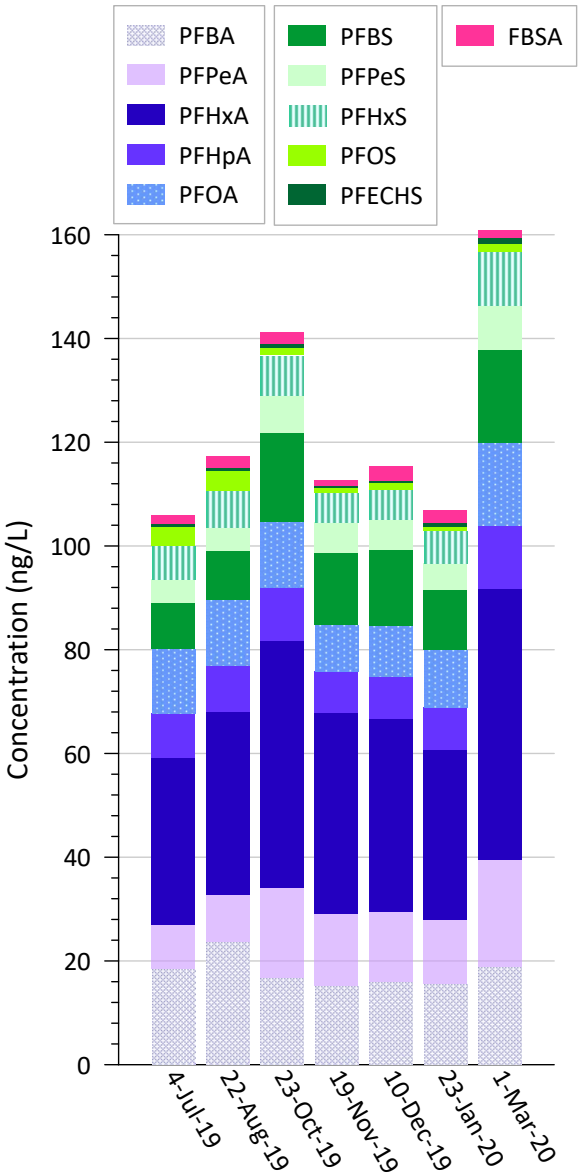

Figure S13. Concentrations of the dominant SC and LC PFAS (maximum > 1 ng/L) measured in the HB outlet stream across seven sample dates.

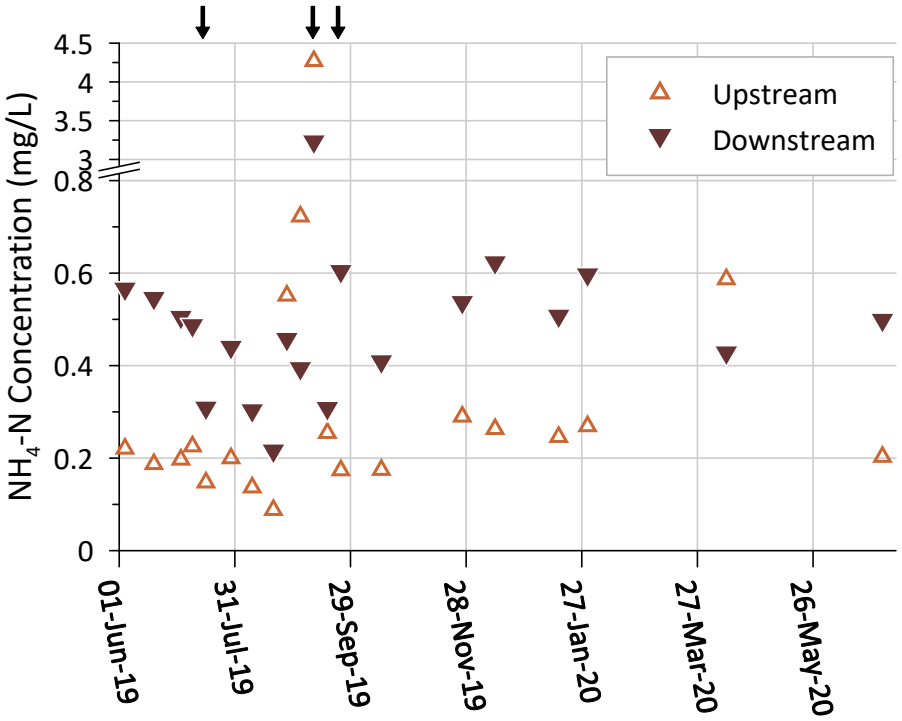

Figure S14. Concentrations of ammonium-N from stream samples collected at the upstream (upward triangle) and downstream (downward triangle) locations along the DC stream (Fig. 1b). Samples were collected during base flow periods but for three at higher flows following a rain event indicated by arrows (at top).

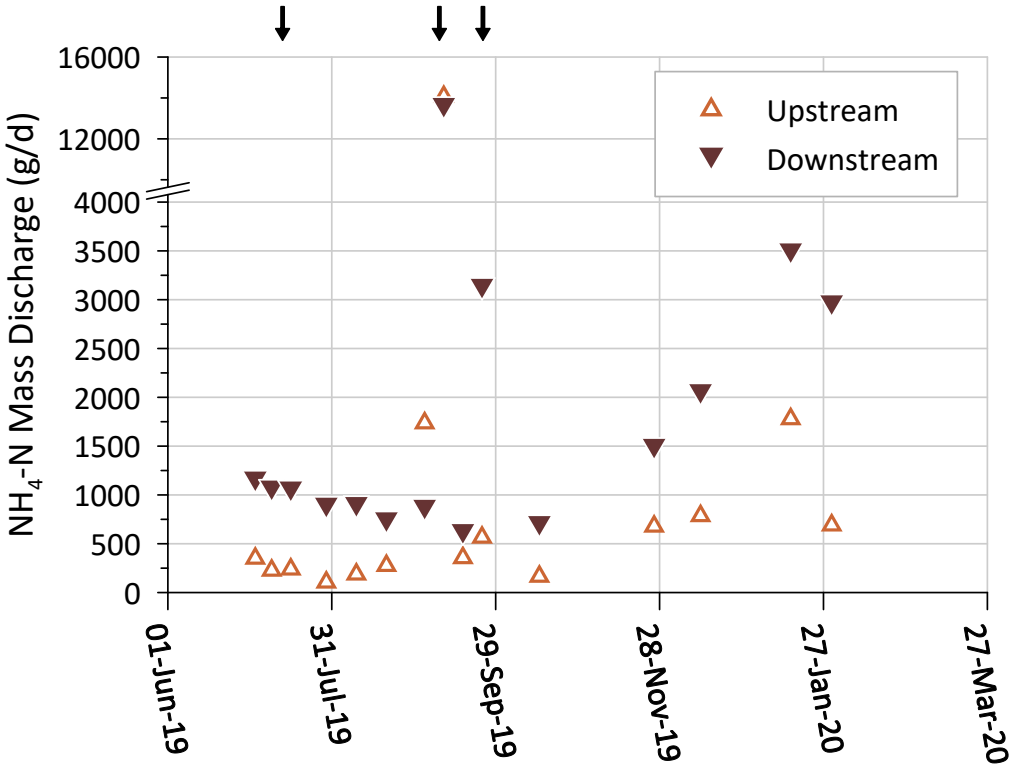

Figure S15. Calculated mass discharge for ammonium-N for the upstream (upward triangle) and downstream (downward triangle) locations along the DC stream (Fig. 1b). Samples were collected during base flow periods but for three at higher flows following a rain event indicated by arrows (at top).

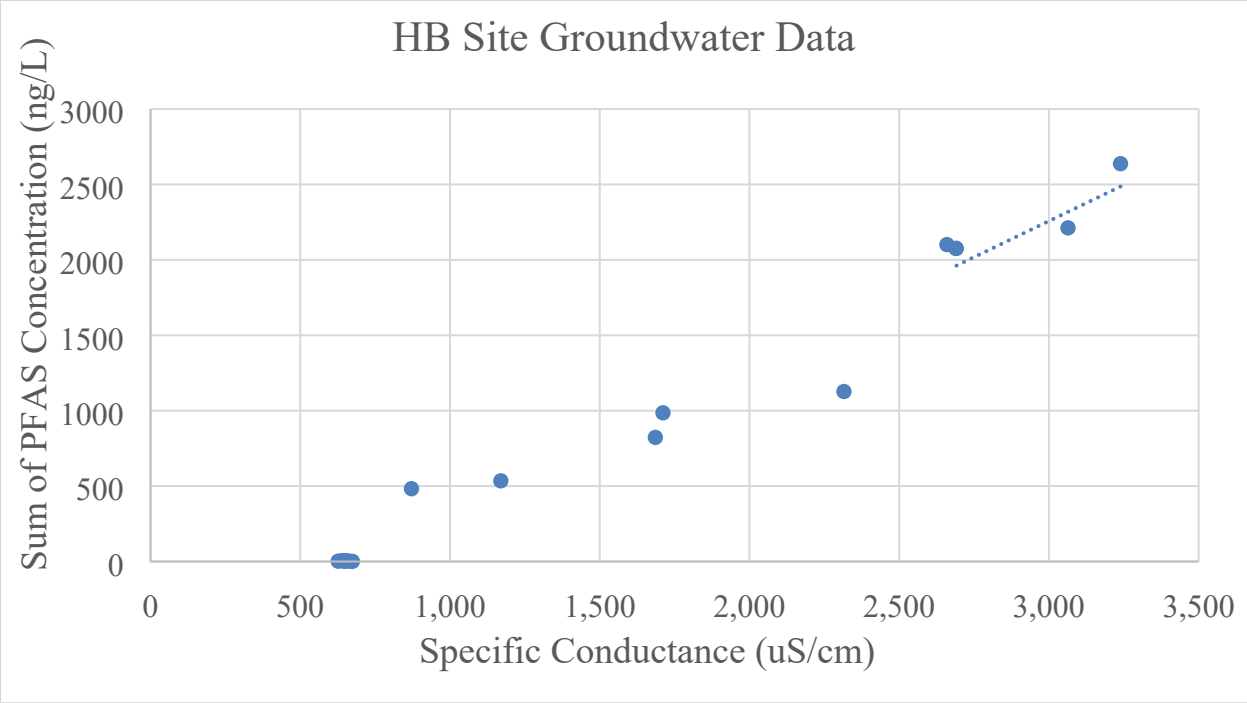

Figure S16. Relationship (linear regression) between the sum of all PFAS concentrations and specific conductance for co-measured groundwater samples from the HB site.

Appendix E: Additional Non-landfill Observations

Other compounds not specific to landfills (Fig. S13), reveal different upstream-downstream concentration patterns. There was no consistent change for acesulfame, which isn't an indicator for historic landfills as it wasn't introduced to markets until the 1990s. It likely reflects inputs of wastewater from leaky sewers (Propp et al. 2022) occurring throughout the city, within and upstream of the landfill reach. Chloride was elevated upstream and showed little change downstream (a few %, up or down; resulting in increased mass discharge with increasing streamflow downstream; not shown), suggesting the stream reach was not only receiving some Cl with contaminated groundwater from the landfill, but also predominantly from road salt (Roy, 2019) and possibly also leaky sewers (Propp et al. 2022), upstream and across the study reach. Finally, though there is limited data (4 dates), concentrations of chlorinated ethenes typically increased dramatically (e.g., from 1 to 55 ug/L for TCE, cis-DCE, VC sum, on one date), but for a higher-flow day, indicating a lack of upstream sources with strong input from a groundwater point source within the area (Roy and Bickerton, 2012).

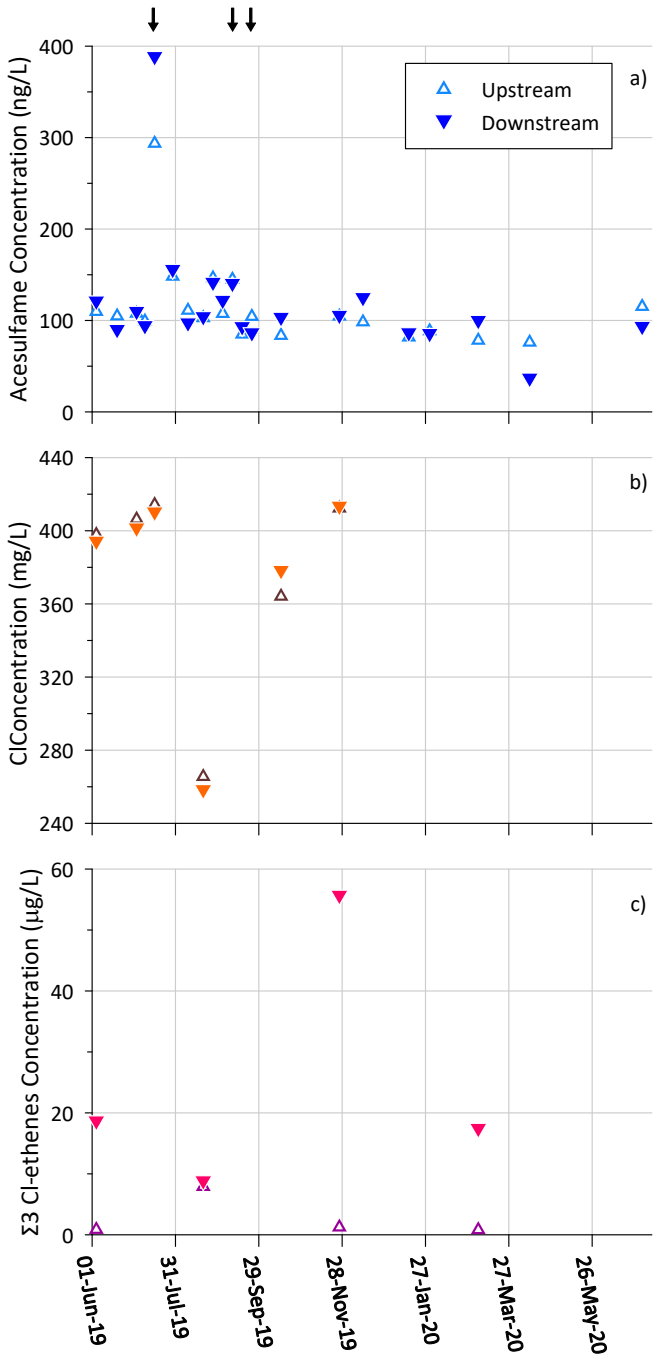

Figure S17. Concentrations of a) artificial sweetener acesulfame, b) chloride, and c) sum of chlorinated ethenes from stream samples collected at the upstream (upward triangle) and downstream (downward triangle) locations along the DC stream (Fig. 1b). Samples were collected during base flow periods but for three at higher flows following a rain event indicated by arrows (at top).

References:

MacInnis, J.J., Lehnherr, I., Muir, D.C.G., St. Pierre, K.A., St. Louis, V.L., Spencer, C., De Silva, A.O. 2019. Fate and Transport of Perfluoroalkyl Substances from Snowpacks into a Lake in the High Arctic of Canada. *Environmental Science and Technology* 53: 10753–10762

Propp VR, Brown SJ, Collins P, Smith JE, Roy JW (2022) Artificial sweeteners identify spatial patterns of historic landfill contaminated groundwater discharge in an urban stream. *Groundwater Monitoring and Remediation* 42(1):50–64. https:// doi. org/ 10. 1111/ gwmr. 12483

Roy, J.W., 2019. Endobenthic organisms exposed to chronically high chloride from groundwater discharging along freshwater urban streams and lakeshores. *Environmental Science & Technology* 53 (16), 9389–9397

Roy, J.W., and G. Bickerton. 2012. Toxic groundwater contaminants: An overlooked contributor to urban stream syndrome? *Environmental Science & Technology* 46, no. 2: 729–736. https://doi.org/10.1021/es2034137

Van Stempvoort, D.R., J. Spoelstra, S.J. Brown, R. Post, and S.A. Smyth. 2019. Sulfamate in environmental waters. *Science of the Total Environment* 695: 133734. https://doi.org/10.1016/j.scitotenv.2019.133734

Van Stempvoort, D.R., Brown, S.J., Spoelstra, J., Garda, D., Robertson, W.D. and Smyth, S.A., 2020. Variable persistence of artificial sweeteners during wastewater treatment: Implications for future use as tracers. *Water Research*, *184*, p.116124.